BIOCHEMISTRY
including biophysical chemistry & molecular biology

Article

pubs.acs.org/biochemistry

# The Tetrameric α-Helical Membrane Protein GlpF Unfolds via a Dimeric Folding Intermediate

Anbazhagan Veerappan,[†,‡] Florian Cymer,[†,‡] Noreen Klein,[†] and Dirk Schneider*[,†]

[†]Institut für Pharmazie und Biochemie, Johannes Gutenberg-Universität Mainz, Johann-Joachim-Becher-Weg 30, 55128 Mainz, Germany

[‡]Institut für Biochemie und Molekularbiologie, ZBMZ, Albert-Ludwigs-Universität, Stefan-Meier-Strasse 17, 79104 Freiburg, Germany

Supporting Information

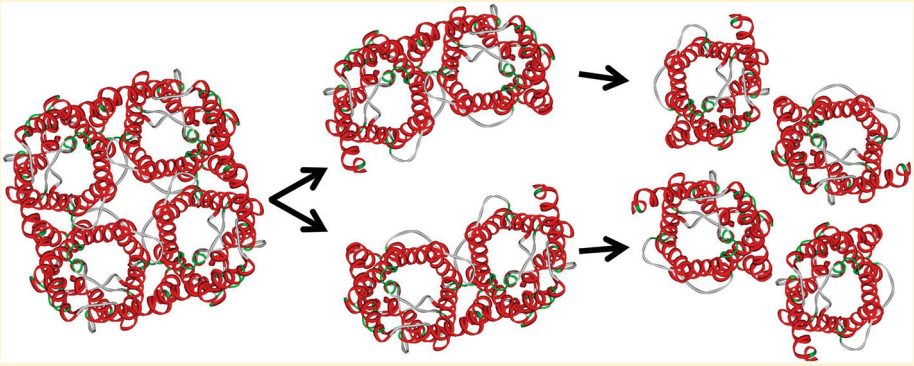

**ABSTRACT:** Many membrane proteins appear to be present and functional in higher-order oligomeric states. While few studies have analyzed the thermodynamic stability of α-helical transmembrane (TM) proteins under equilibrium conditions in the past, oligomerization of larger polytopic monomers has essentially not yet been studied. However, it is vital to study the folding of oligomeric membrane proteins to improve our understanding of the general mechanisms and pathways of TM protein folding. To investigate the folding and stability of the aquaglyceroporin GlpF from *Escherichia coli*, unfolding of the protein in mixed micelles was monitored by steady-state fluorescence and circular dichroism spectroscopy as well as by seminative sodium dodecyl sulfate−polyacrylamide gel electrophoresis analyses. On the basis of our results, it appears most likely that GlpF unfolds in a two-step process, involving the equilibrium of tetrameric, dimeric, and monomeric GlpF species. A kinetic analysis also indicates an intermediate along the kinetic GlpF unfolding pathway, and thus, two phases are involved in GlpF unfolding. While three-state unfolding pathways and a dimeric folding intermediate are not uncommon for water-soluble proteins, a stable (un)folding intermediate with a decreased oligomeric structure has not been detected or reported for any α-helical membrane protein.

Membrane proteins are encoded by up to one-third of the human genome,[1] and almost 50% of all currently available drugs target membrane proteins.[2] However, folding of membrane proteins is still poorly understood. Information about protein folding pathways is frequently derived from protein unfolding studies, as proteins are typically isolated from an organism in a natively folded state. While some denaturants that are well-established for studying (un)folding pathways of water-soluble proteins, these can usually not be used to study (un)folding pathways of membrane proteins,[3] as, for example, typically only subtle structural changes can be observed even at high urea and guanidinium hydrochloride concentrations.[4] Moreover, membrane proteins can structurally be highly stable at elevated temperatures and tend to suddenly aggregate at a certain temperature, which greatly limits the information that can be gained by thermal denaturation studies. In addition, studying unfolding of the membrane integral parts of a protein can also be complicated by the fact that membrane proteins often contain larger soluble domains besides the transmembrane (TM) regions, and thus, unfolding of different domains has to be depicted.

Approximately a decade ago a technique that allows the study of unfolding of α-helical membrane proteins in vitro was introduced.[5] Addition of a harsh detergent [typically sodium dodecyl sulfate (SDS)] to a membrane protein solubilized in a mild detergent [e.g., *n*-dodecyl β-D-maltoside (DDM)] results in formation of mixed DDM/SDS micelles, which causes progressive unfolding of the protein. In contrast to soluble proteins, SDS denaturation does usually not result in complete unfolding of a polypeptide chain;[6] SDS rather induces dissociation of TM helices without dramatically altering their secondary structure.[7] Thus, in the case of α-helical membrane

**Received:** August 11, 2011
**Revised:** October 28, 2011
**Published:** October 28, 2011

  

proteins, the term "unfolding" is mostly used to describe SDS-induced TM helix–helix dissociation. Mixed DDM/SDS micelles have been used several times in the past to study unfolding of membrane proteins,[5,8−10] but only very recently were some aspects of the principles guiding unfolding of an $\alpha$-helical membrane protein investigated in greater detail.[11,12] While some details of TM protein (un)folding have been studied in recent years, several aspects of TM protein folding have not yet been considered. It is, for example, still largely mysterious how, when, and why many TM proteins form higher-order oligomers while the monomer represents the functional unit, though TM protein oligomers appear to be highly important for proper protein function.

Aquaporins are polytopic membrane proteins that facilitate a rapid flux of water across different cellular membranes.[13] They occur in all kingdoms of life, and in the human genome, 13 different aquaporins are encoded. Among them are also members of the subfamily of aquaglyceroporins that facilitate not only the flux of water across cellular membranes but also the flux of polyalcohols, such as glycerol.[14] All aquaporins share a highly conserved structure, and it is generally assumed that all aquaporins form tetramers. Oligomerization of individual aquaporin monomers has been observed in detergents as well as in a membrane environment.[15,16] Furthermore, recent observations indicate that the function of the bacterial aquaglyceroporin GlpF depends on its oligomeric state.[17] The structure of the *Escherichia coli* aquaglyceroporin GlpF was determined a decade ago,[18] and because the structure and function of GlpF have been studied to a much greater extent than their human counterparts, GlpF became a paradigm for studying the folding, structure, and functions of aquaglyceroporins. While the stability of some aquaporins has been analyzed to some extent[19,20] and while a few specific features of the human AQP1 folding pathway have been analyzed,[21] details of the folding pathway of aquaporins and of aquaglyceroporins are still elusive; in particular, formation of the tetrameric structure has not yet been studied. Thus, studying unfolding of GlpF offers the unique opportunity to gain for the very first time detailed insights into the formation and function of membrane protein oligomers.

In this study, we monitored unfolding of the *E. coli* GlpF protein in mixed DDM/SDS micelles. The unfolding pathway of the GlpF protein was systematically followed on the level of quaternary, tertiary, and secondary structure. On the basis of our results, we conclude that unfolding of the tetrameric GlpF to the GlpF monomers involves formation of a stable dimeric intermediate folding state.

## EXPERIMENTAL PROCEDURES

**Expression and Purification of *E. coli* GlpF.** Molecular cloning, protein expression, and purification were conducted as previously described.[17] The protein concentration was determined by measuring the absorbance at 280 nm using the calculated molar extinction coefficient of 38305 $M^{-1}$ $cm^{-1}$.[16] The protein concentration was adjusted to the desired concentrations by adding different volumes of 10 mM phosphate buffer (pH 8.0) and 5 mM DDM.

**Equilibrium Unfolding.** DDM and SDS were obtained from Sigma-Aldrich (Munich, Germany). The unfolding transitions of GlpF were monitored by measuring circular dichroism (CD) and Trp fluorescence. CD measurements were taken at 25 °C in a JASCO J-815 spectropolarimeter at a scan speed of 20 nm/min using 0.1 cm path-length quartz cells. Far-UV CD spectra were recorded as described above. The intensity and the wavelength of the CD spectrometer were calibrated using *d*-10-camphosulfonic acid.[22] Data were collected with a response time of 2 s and a slit width of 1 nm. Each reported spectrum was the average of at least three consecutive scans, from which buffer scans, recorded under the same conditions, were subtracted. The measured ellipticity was converted to mean residue ellipticity by

$$\text{mean residue ellipticity (MRE)} = 100\,\theta/(cnl) \quad (1)$$

where $\theta$ is the measured ellipticity in millidegrees, $c$ is the protein concentration in micromolar, $n$ is the number (304) of residues, and $l$ is the path length in centimeters.[23] All CD spectra were analyzed using CDPro. The helicity was estimated by using the CDSSTR algorithm and a reference data set (number 10) containing both soluble proteins and membrane proteins. The change in the ratio of the mean residue ellipticity at 208 and 222 nm was used to monitor the unfolding transition.

Equilibrium unfolding was initiated by adding increasing amounts of SDS to GlpF in 5 mM DDM and 10 mM phosphate buffer (pH 8.0). Mole fractions were used throughout the experiment. Mole fractions were obtained from the total detergent concentrations rather than some estimate of concentrations in micelles, as it is difficult to distinguish between free SDS and SDS present in mixed micelles in this mixture.[10] Prior to measurement, each sample was incubated at room temperature for 30 min.

Fluorescence emission spectra were measured in a Thermo Spectronic Aminco Bowman Series 2 luminescence spectrometer using excitation and emission wavelength set to 280 and 325 nm, respectively. The decrease in Trp fluorescence at 325 nm was recorded to follow GlpF unfolding.

SDS-induced equilibrium unfolding of GlpF was analyzed by a three-state model (details in the Supporting Information)

$$T_4 \overset{K_1}{\leftrightarrow} 2D_2 \overset{K_2}{\leftrightarrow} 4U \quad (2)$$

where T, D, and U represent the tetramer, dimer, and monomer/partially unfolded monomer, respectively.

**Seminative Polyacrylamide Gel Electrophoresis Analysis.** To minimize the amount of SDS present during sodium dodecyl sulfate–polyacrylamide gel electrophoresis (SDS–PAGE), SDS was omitted from the sample buffer and was included in only the running buffer and the gels (3.46 mM SDS), because a high SDS concentration in the sample buffer (60 mM) would significantly lower the sensitivity of this method. At 3.46 mM SDS, GlpF is still largely tetrameric, which is assumed to represent the natively folded quaternary structure. Prior to seminative SDS–PAGE, samples were incubated at room temperature for 15 min.[24] SDS–PAGE gels were stained with Coomassie dye, and bands were quantified using Scion Image (Scion Corp.).

**Size Exclusion Chromatography.** Monomeric, dimeric, and tetrameric GlpF were separated by size exclusion chromatography at room temperature on a BioSep-SEC-S4000 column (Phenomenex, Torrance, CA) using an Äkta Basic liquid chromatograph (GE Healthcare, Munich, Germany) at a flow rate of 1 mL/min. The column was equilibrated with buffer [10 mM sodium phosphate (pH 8.0), 5 mM DDM, and 20 mM SDS]. Fractions (250 $\mu$L) were collected and analyzed by SDS–PAGE.

**Kinetic Unfolding Experiments.** Kinetics of GlpF unfolding were measured at 25 °C with an SX20 stopped-flow instrument (Applied Photophysics Inc.). Typically, GlpF in 5 mM DDM was mixed rapidly with an equal volume of SDS. Time-resolved Trp fluorescence emission was followed at 325 nm directly by using a second programmable monochromator. Kinetic traces were analyzed using the Pro-K global analysis software provided by the manufacturer.

## RESULTS

**Unfolding of GlpF Monitored by Trp Fluorescence and CD Spectroscopy.** To analyze the unfolding pathway of the *E. coli* aquaglyceroporin GlpF, we monitored the protein secondary structure by CD spectroscopy during unfolding of the GlpF tetramer by SDS. As GlpF contains five Trp residues in the TM domain, we additionally followed changes in the GlpF tertiary (and quaternary) structure by fluorescence spectroscopy. To first define the optical properties of native and SDS-unfolded GlpF, we measured Trp fluorescence and CD spectra using GlpF in 5 mM DDM micelles (native state) as well as denatured GlpF in mixed micelles containing 5 mM DDM and 100 mM SDS (expressed throughout as bulk mole fraction SDS, $\chi_{SDS}$). After Trp excitation, native GlpF had a fluorescence emission maximum at 325 nm, indicating that the five Trp residues are buried within a highly hydrophobic environment. Addition of SDS ($0.95\chi_{SDS}$) and formation of mixed DDM/SDS micelles resulted in a 3 nm red shift of the fluorescence emission maximum and an ~37% decrease in the fluorescence intensity at 325 nm (Figure 1A). This indicates that the structure of the GlpF tetramer differs significantly in pure DDM and mixed DDM/SDS micelles, whereas solvent exposure of the Trp residues changes only moderately. A 10-fold dilution of GlpF in buffer without SDS results in refolding of the protein and in a fluorescence spectrum similar to the spectrum of GlpF in pure DDM micelles. The far-UV CD spectra of GlpF in 5 mM DDM at $0.95\chi_{SDS}$ are shown in Figure 1B, together with the spectrum of GlpF after refolding. Native GlpF exhibited a CD spectrum typical for an $\alpha$-helical protein, having minima at 208 and 222 nm. While the characteristic minima are still pronounced at $0.95\chi_{SDS}$, a decreased mean residue ellipticity (MRE) of the double minima was observed. Calculation of the secondary structure content, using CDPro, suggested a content of $\alpha$-helices, turns, and random coils of 67, 12, and 21%, respectively, in 5 mM DDM. At $0.95\chi_{SDS}$, the secondary structure composition had changed significantly to 57, 17, and 26%, indicating partial unfolding of the GlpF protein at high SDS concentrations, which was already evident from the decrease in the minima at 208 and 222 nm (Figure 1B). It is noteworthy that while alterations of the secondary structure can be monitored by CD spectroscopy, the predicted content of the individual secondary structure elements must be taken with some care, as the reference data set contains both soluble and TM proteins (see Experimental Procedures). As GlpF contains only small soluble loop regions and because all $\alpha$-helices are essentially membrane-integrated, changes in the helicity likely originate from structural alterations in the TM domain. Taken together, these results suggest partial unfolding of GlpF in mixed micelles, and unfolding can be monitored by fluorescence as well as by CD spectroscopy.

**Equilibrium Unfolding.** To determine the free energy of unfolding, native GlpF (in DDM) was incubated at a range of SDS concentrations until equilibrium was reached. Both Trp fluorescence and the CD signal at 222/208 nm were used to determine the fraction of unfolded GlpF. Apparent changes in the Trp fluorescence emission as well as in the CD signal are plotted versus $\chi_{SDS}$ in Figure 2. The observed changes in the fluorescence and CD signals indicate that unfolding of GlpF involves two transitions with different midpoints ($C_m$), as summarized in Table 1. Thus, unfolding of GlpF in mixed micelles appears to involve formation of a distinct intermediate structure.

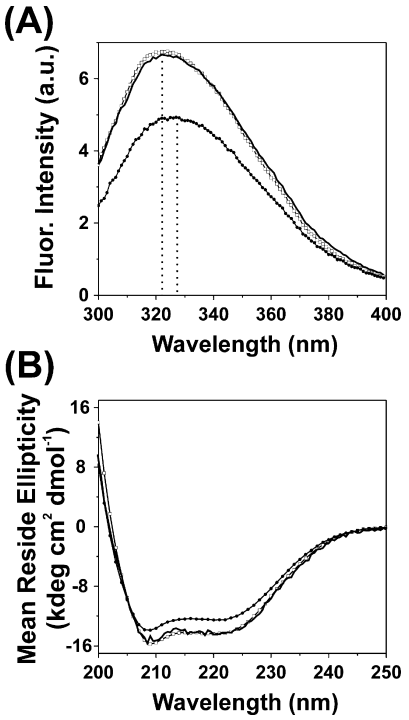


**Figure 1.** Steady-state fluorescence and CD analysis of GlpF unfolding. (A) Changes in GlpF intrinsic fluorescence during unfolding and refolding in mixed micelles were monitored with 5 $\mu$M GlpF in 5 mM DDM (□), GlpF unfolded at $0.95\chi_{SDS}$ (●), and GlpF refolded from mixed micelles at $0.85\chi_{SDS}$ by 10-fold dilution into buffer containing solely 5 mM DDM (—). (B) Far UV-CD spectra of native (□) and unfolded GlpF at $0.95\chi_{SDS}$ (●), as well as of GlpF refolded from mixed micelles at $0.85\chi_{SDS}$ by 10-fold dilution into buffer containing solely 5 mM DDM (—).

To confirm the presence of a stable (un)folding intermediate, we next performed a seminative SDS–PAGE analysis. As GlpF retains the native tetrameric structure on SDS gels,[16,17] SDS–PAGE is a powerful tool for studying the oligomeric state of GlpF. GlpF unfolding was followed by SDS–PAGE after incubaton of the native GlpF tetramer at various $\chi_{SDS}$ values (Figure 3A), which results in continuous disassembly of the native protein structure. Noteworthy is the fact that the presence of SDS in the electrophoresis buffer (~3.5 mM) already caused slight unfolding and/or disassembly of GlpF, resulting in a faint dimeric band, as visible in the first lane in Figure 3. Nevertheless, the band intensity of the dimeric and the monomeric GlpF steadily increased with an increasing $\chi_{SDS}$. At $\chi_{SDS}$ values of >0.80, the ratio of the dimeric and monomeric GlpF does not appear to change further in the SDS gel analysis, and thus, complete monomerization of the dimer cannot be observed under the specific conditions needed to perform the SDS–PAGE analysis. However, the SDS–PAGE analysis strongly indicates that the GlpF tetramer dissociates to a monomeric state via a dimeric intermediate that can be visualized on SDS gels. Quantification of the intensity of the

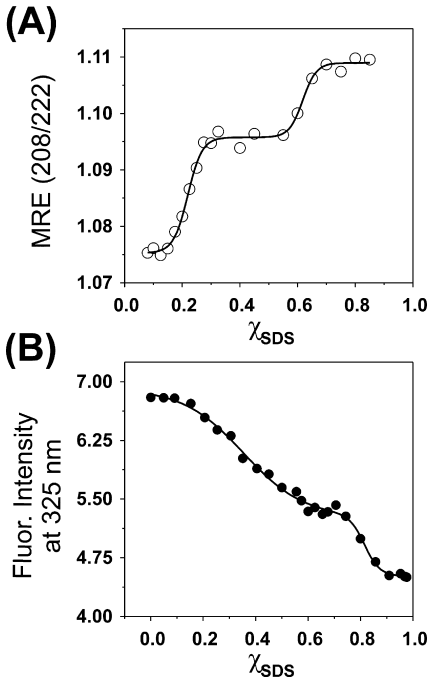


**Figure 2.** Equilibrium unfolding of GlpF. (A) GlpF unfolding monitored by CD spectroscopy in the far-UV region as shown in Figure 1B, and the 208 nm/222 nm ratio was plotted vs $\chi_{SDS}$. (B) Trp fluorescence at 325 nm measured as specified in the legend of Figure 1A at various $\chi_{SDS}$ values and plotted vs $\chi_{SDS}$. The solid line represents the best fit obtained using the three-state model described in the text. The protein concentration used in both measurements was 5 $\mu$M.

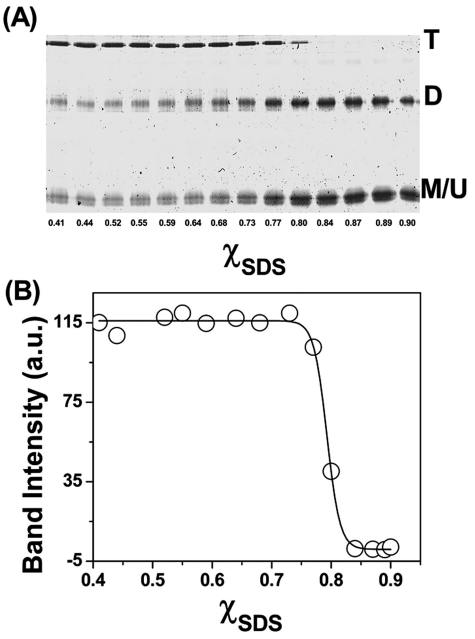


**Figure 3.** Seminative SDS–PAGE analysis and dissociation of wild-type GlpF into its subunits by increasing SDS concentrations. (A) Representative Coomassie Blue-stained gel, in which the tetrameric (T), dimeric (D), and monomeric or partially unfolded (M/U) forms of GlpF are indicated. The $\chi_{SDS}$ values were 0.41, 0.44, 0.52, 0.55, 0.59, 0.64, 0.68, 0.73, 0.77, 0.80, 0.84, 0.87, 0.89, and 0.90. (B) Band intensity of the tetrameric GlpF species plotted vs $\chi_{SDS}$. GlpF samples, at a protein concentration of 5 $\mu$M, in 10 mM phosphate buffer (pH 8.0) containing 5 mM DDM were treated with SDS for 15 min to the final $\chi_{SDS}$ and then mixed with sample buffer devoid of SDS and loaded onto a 12% acrylamide gel.

GlpF tetramer band on the SDS gels after incubation of the protein at various $\chi_{SDS}$ values showed that the tetramer dissociates completely at a $\chi_{SDS}$ of >0.8 (Figure 3B).

To further evaluate whether dimeric GlpF represents a stable unfolding intermediate, we next analyzed the GlpF oligomeric structure at a $\chi_{SDS}$ of 0.8 by size exclusion chromatography. As one can see in Figure 4, in mixed micelles three GlpF species with distinct sizes elute from the size exclusion column. As indicated by the SDS–PAGE analysis, the three peaks correspond to monomeric, dimeric, and tetrameric GlpF, respectively. Thus, the dimeric GlpF species represents a distinct and stable GlpF (un)folding intermediate.

On the basis of our experimental results, GlpF unfolding appears to involve two steps, a three-state model involving a dimeric intermediate was used to analyze the GlpF unfolding data summarized in Figure 2, and the results of the fluorescence and CD measurements were fitted to the $T_4 \leftrightarrow 2D_2 \leftrightarrow 4U$ model (eq 2). While we also tried to fit the data to a simpler two-state model ($T_4 \leftrightarrow 4U$), the quality of such fits was poor, and this analysis was not considered any further. The overall free energy of GlpF unfolding in the absence of a denaturant ($\Delta G^{\circ}_{tot}$) was determined to be 16.41 kcal/mol. The *m* values, which are related to changes in solvent exposure from the native to the denatured state, were 8.90 and 16.92 kcal/mol for the first and second transitions, respectively. These values indicate that during the first $T_4 \leftrightarrow 2D_2$ transition, fewer parts of the GlpF protein structure are exposed to the solvent environment than after the $2D_2 \leftrightarrow 4M$ transition. To obtain these overall free energy values associated with the unfolding reaction of GlpF, we assumed that the unfolding reaction was near equilibrium. This assumption was supported by the observations that the unfolded protein refolded after dilution, because the Trp fluorescence and the CD signal recovered to wild-type levels when denatured GlpF ($0.85\chi_{SDS}$) was diluted 10-fold in buffer containing only 5 mM DDM (Figure 1). In this experiment, the final protein concentration was similar to the concentrations used in the un- and refolding experiments shown in Figure 1. Furthermore, refolding of the protein and reappearance of the GlpF tetramer were also monitored by

**Table 1. Thermodynamic Parameters As Determined by Equilibrium Experiments**[a]

| | transition midpoints, $\chi_{SDS}$ | | | | | |
|---|---|---|---|---|---|---|
| | $C_{m1}$ | $C_{m2}$ | $\Delta G_{T-D}$ (kcal/mol) | $-m_{T-D}$ (kcal/mol) | $\Delta G_{D-U(M)}$ (kcal/mol) | $-m_{D-U(M)}$ (kcal/mol) |
| fluorescence | 0.36 | 0.80 | 2.60 | 8.90 | 13.81 | 16.92 |
| CD | 0.22 | 0.60 | 1.46 | 7.39 | 10.18 | 15.98 |

[a]The parameters were calculated on the basis of the experimental data shown in Figure 2. Noteworthy, as discussed in the text, is the fact that fluorescence and CD spectroscopy monitor different structural alterations.

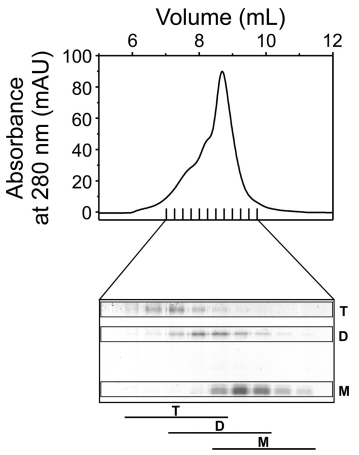


**Figure 4.** Elution profile of GlpF from a gel filtration column in buffer containing a $\chi_{SDS}$ of 0.8. A chromatogram of isolated GlpF in buffer with a $\chi_{SDS}$ of 0.8 indicates three GlpF species with distinct sizes. Absorbance was recorded at 280 nm. Analysis of the corresponding fractions by SDS–PAGE (bottom) indicates that the three species represent tetrameric (T), dimeric (D), and monomeric (M) GlpF. Fractions, in which the respective oligomeric GlpF forms elute, are marked.

seminative SDS–PAGE (Figure 5), which further confirmed the reversibility of SDS-induced GlpF unfolding.

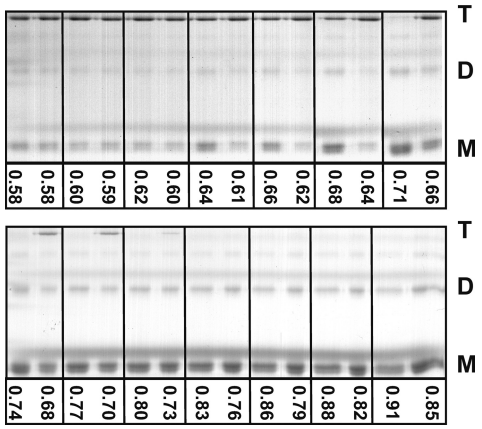


**Figure 5.** Refolding of the GlpF quaternary structure monitored by seminative SDS–PAGE. In each box, lane 1 contained the denatured sample and lane 2 the sample refolded from the $\chi_{SDS}$ of the sample in lane 1. Two aliquots were taken. To one aliquot 1 volume of 5 mM DDM was added, and to the other 1 volume of 5 mM DDM in buffer (pH 8.0) containing the final concentration of SDS as in the original GlpF/SDS mixture. These aliquots were incubated at room temperature for 15 min, and seminative SDS–PAGE was performed as described. All mole fractions given account also for the SDS present in the running buffer and the gels.

**Structural Alterations Preceding Subunit Dissociation.** To further define individual steps eventually preceding tetramer dissociation, we monitored the thermal stability and structural flexibility of GlpF at different $\chi_{SDS}$ values by far-UV CD spectroscopy (Figure S1A of the Supporting Information). An isodichroic point appeared at 201 nm at all tested $\chi_{SDS}$ values, indicating that a two-state transition is occurring.[25] While the CD and fluorescence spectra remained unchanged between 0 and 0.15$\chi_{SDS}$, which indicates a stable protein structure, the unfolding transition temperature ($T_m$) monitored at 0.15$\chi_{SDS}$ was decreased to 67 °C compared to the $T_m$ of the protein in 5 mM DDM (~70 °C). The $T_m$ further decreased steeply upon addition of increasing SDS concentrations (Figure S1 of the Supporting Information). These results indicate that, while the GlpF protein structure is well preserved under nondenaturing conditions, already low SDS concentrations destabilize the GlpF structure locally, resulting in the observed decreased $T_m$.

**Stopped-Flow Fluorescence Kinetic Measurement.** The kinetics of GlpF unfolding was followed by monitoring changes in the Trp fluorescence using a stopped-flow fluorescence spectrometer. When GlpF was rapidly mixed with various SDS concentrations, a decrease in the Trp fluorescence intensity caused by the partial GlpF unfolding was monitored, until equilibrium was reached (Figure 6A).

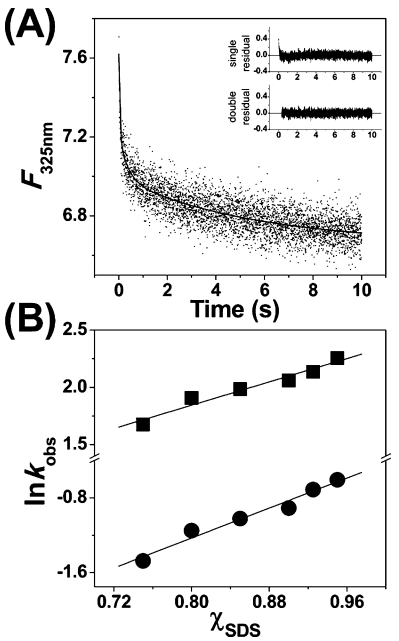


**Figure 6.** Stopped-flow fluorescence kinetics of GlpF unfolding in mixed micelles. Native GlpF (15 $\mu$M) in 5 mM DDM was mixed rapidly with an equal volume of SDS to a final $\chi_{SDS}$ of 0.95. (A) Kinetic trace of dissociation of the GlpF tetramer at 0.95$\chi_{SDS}$. The inset shows residuals after using single-exponential (top) and double-exponential (bottom) fits for data analysis. The latter fit resolved rate constants for the fast and slow phases. (B) Dependence of rate constants $k_1$ [fast phase (■)] and $k_2$ [slow phase (●)] on $\chi_{SDS}$. Data were analyzed by PC Pro-K global analysis software and fitted with a biexponential function (—). $m_u$ is the sensitivity of $k_u$ to $\chi_{SDS}$ (eq 3): 2.54 and 4.01 for fast and slow phases, respectively.

Refolding of GlpF was followed by stopped-flow spectroscopy by dilution of a GlpF-containing solution with a high $\chi_{SDS}$ to reduce the final SDS concentration (Figure S2 of the Supporting Information), which further demonstrates the reversibility of the unfolding process. However, at the high protein concentrations needed for the refolding experiments, GlpF tended to aggregate and, as the signal could no longer be properly followed using a second monochromator, the signal-to-noise ratio and the quality of the signals were severely reduced, which influenced the analyses of data. Therefore, single-wavelength measurements were used for determining unfolding rates, as described in Experimental Procedures. Changes in the fluorescence intensities caused by GlpF

unfolding, as, for example, shown in Figure 6A, were fitted using a double-exponential function representing two unfolding rates: a fast phase with a rate constant $k_{u1}$ of 7.28 $s^{-1}$ and a slow phase with a rate constant $k_{u2}$ of 0.36 $s^{-1}$ at $0.85\chi_{SDS}$. Fitting the data to a sum of three exponential functions did not improve the residual plot further. Thus, unfolding of GlpF in mixed micelles involves (at least) two kinetic processes, which is in excellent agreement with the equilibrium measurements described above (Figure 2).

Because $\ln(k)$ is linear with respect to $\chi_{SDS}$ for $k_{u1}$ and $k_{u2}$, the unfolding data were further analyzed using the following equation:

$$\ln(k_u) = \ln(k^0) + m\chi_{SDS} \quad (3)$$

where $k_u$ is the rate constant, $k^0$ is the rate constant in the absence of SDS, $\chi_{SDS}$ is the SDS mole fraction, and $m$ is a constant, in accordance with the equilibrium constant of unfolding.

Unfolding kinetics were monitored at different $\chi_{SDS}$ values (Figure 6B), and extrapolation of the data to the $y$-axis provided unfolding rates in the absence of SDS of 0.83 and $11.85 \times 10^{-3}$ $s^{-1}$ for the fast ($k_1$) and slow ($k_2$) phases, respectively.

## DISCUSSION

While folding and stability are well analyzed and described for many water-soluble proteins, only few studies have analyzed the thermodynamic stability of $\alpha$-helical TM proteins under equilibrium conditions.[5,9,10,26] To improve our understanding of the general mechanisms and pathways of TM protein folding, it is vital to study folding of oligomeric membrane proteins, because many membrane proteins appear to be present and functional in a higher-order oligomeric state, where the subunits are held together by noncovalent interactions. However, oligomerization of folded TM protein monomers has not been considered in most studies analyzing the folding pathways and stability of TM proteins. Only very few studies consider and discuss TM protein oligomerization, as, for example, the studies describing the folding and stability of the trimeric *E. coli* DAGK (e.g., ref 27) or the tetrameric *Streptomyces lividans* KcsA protein.[28] Furthermore, recently, unfolding of the soluble parts of an oligomeric TM protein has been studied in greater detail,[26,29] which marks an important initial step in gaining an in-depth understanding of the structural stability of oligomeric TM proteins. In this study, we have used GlpF to study unfolding of a large oligomeric TM protein. On the basis of the GlpF crystal structure, the glycerol-conducting channel is located in the center of each GlpF monomer,[18] yet the formation of the tetramer appears to be vital for proper GlpF channel function.[17] In recent years, mixed SDS/DDM micelles have emerged as a powerful tool for studying the thermodynamic stability of $\alpha$-helical TM proteins,[5,7,9,10] and in this study, we have used mixed micelles to investigate the folding and stability of the aquaglyceroporin GlpF. By combining results from steady-state fluorescence and CD measurements with seminative SDS–PAGE analyses, we demonstrate that GlpF unfolding cannot be described by a simple two-state mechanism. On the basis of our results, it appears most likely that GlpF unfolds in a two-step process, involving equilibrium of a tetrameric, a dimeric, and a monomeric GlpF species, and the dimeric GlpF represents a distinct and stable (un)folding intermediate (Figure 4). The unfolding kinetics shown in Figure 6 suggest that two phases are involved in GlpF unfolding, which also indicates an intermediate along the kinetic GlpF unfolding pathway. While three-state unfolding pathways and a dimeric folding intermediate are not uncommon for water-soluble proteins,[30,31] a stable (un)folding intermediate with a decreased oligomeric structure has not been detected or reported for any $\alpha$-helical membrane protein before.

**Intermediate State.** According to the observed thermal stabilities (Figure S1 of the Supporting Information), the dimeric (un)folding intermediate probably has a reduced level of tertiary structure, whereas the secondary structure is mostly conserved (Figure 2A), which in part resembles intermediate states assumed for folding of globular proteins.[32] As was observed in the equilibrium unfolding experiments, the $m$ value of the $T_4 \leftrightarrow 2D_2$ transition was lower than that of the second $D_2 \leftrightarrow 2M$ transition (Table 1), indicating that only a fraction of the buried surface area is exposed at the subunit interface after the first transition, whereas the entire subunit interface is exposed after the second transition. This assumption is further supported by the seminative SDS–PAGE analyses (Figure 3), which clearly show the $2D_2 \leftrightarrow 4U$ transition occurring at SDS concentrations exceeding $0.8\chi_{SDS}$. These results suggest that the (un)folding intermediate has a structure distinct from the native tetramer and the unfolded protein monomer. On the basis of the results of the equilibrium, SDS–PAGE, and thermal stability studies, we suggest that during GlpF (un)folding a dimeric GlpF intermediate appears; its structure is not as tightly packed as that of the natively folded tetrameric GlpF.

**Overall Stability of GlpF.** Although the number of studies reporting equilibrium unfolding of membrane proteins is limited, we compare the few available literature values with our results to evaluate the stability of the GlpF tetramer. The total Gibbs free energy of GlpF unfolding in the absence of SDS ($\Delta G^\circ_{tot}$) is 16.41 kcal/mol. The free energies determined by SDS unfolding of bacterorhodopsin (bR) in DMPC and CHAPS micelles and the *E. coli* diacylglycerol kinase (DAGK) TM domain in decylmaltoside are ~20[9] and ~16 kcal/mol, respectively, which is in good agreement with the values determined for GlpF in this study. Reversible unfolding of a detergent-solubilized tetrameric KcsA protein by 2,2,2-trifluoroethanol yielded a $\Delta G$ value of approximately 30 kcal/mol, which is slightly higher than the values obtained with other oligomeric TM proteins by SDS-induced denaturation.[28] The high stability of GlpF (and of other TM proteins) mostly arises due to subunit–subunit interaction and formation of the quaternary structure. In line with this, the crystal structure of the GlpF monomer is highly stabilized at the monomer–monomer interface, as is evident from the local $B$ factors,[18] which describe the structural flexibility of a given protein region. It is also reasonable to assume that the oligomeric nature of GlpF contributes to its higher stability, as monomeric proteins require fewer SDS molecules than the oligomeric protein to induce unfolding. The $\Delta G^\circ_{tot}$ value of 4.4 kcal/mol obtained after unfolding of the disulfide bond reducing protein B (DsbB) from *E. coli* is in line with such an assumption, as DsbB appears to be monomeric.[10] In contrast, the three membrane proteins with higher determined $\Delta G^\circ_{tot}$ values, GlpF,[18] bR,[33] and DAGK,[34] are known to form oligomers.

**Conclusion.** Previously, it has been shown that oligomerization of the aquaglyceroporin GlpF significantly influences its activity.[17] In this study, we show that unfolding of the native tetramer in mixed micelles involves formation of a distinct

dimeric folding intermediate, and the dimeric intermediate refolds to the native tetrameric state. On the basis of our results, we can essentially rule out a sequential addition of monomers to form the tetrameric state (where two intermediates should be present), at least in vitro. To the best of our knowledge, this is the first study in which a distinct folding intermediate with a lower-order oligomeric state (dimer vs tetramer) has been identified during the unfolding and refolding of a large $\alpha$-helical TM protein. Our results clearly suggest that formation of the GlpF quaternary structure proceeds from a monomer to a dimer and two dimers then form a tetramer. It is likely that also in vivo, within a biological membrane, GlpF assembles via the described dimeric folding intermediate.

## ■ ASSOCIATED CONTENT

### Ⓢ Supporting Information

Equilbrium unfolding data analysis, GlpF thermal unfolding monitored by changes in secondary structure (Figure S1), and stopped-flow fluorescence kinetics of GlpF refolding (Figure S2). This material is available free of charge via the Internet at http://pubs.acs.org.

## ■ AUTHOR INFORMATION


### Corresponding Author

*Department of Pharmacy and Biochemistry, Johannes Gutenberg-University Mainz, Johann-Joachim-Becher-Weg 30, 55128 Mainz, Germany. Phone: +49 6131 39-25833. Fax: +49 6131 39-25348. E-mail: Dirk.Schneider@uni-mainz.de.

### Author Contributions

A.V. and F.C. contributed equally to this work and are listed in alphabetical order.



### Funding

D.S. is supported by grants from the Stiftung Rheinland-Pfalz für Innovation, the Deutsche Forschungsgemeinschaft (SCHN 690/2-3 and GRK 1478), the German-Israeli Foundation, the Research Center "Complex Materials" (COMATT), and the University of Mainz.


## ■ ACKNOWLEDGMENTS

We thank Annette Roth for excellent technical assistance and Hildegard Pearson for carefully proofreading the manuscript.

## ■ REFERENCES


(1) Fagerberg, L., Jonasson, K., von Heijne, G., Uhlen, M., and Berglund, L. (2010) Prediction of the human membrane proteome. *Proteomics 10*, 1141−1149.

(2) Hopkins, A. L., and Groom, C. R. (2002) The druggable genome. *Nat. Rev. Drug Discovery 1*, 727−730.

(3) Bowie, J. U. (2005) Solving the membrane protein folding problem. *Nature 438*, 581−589.

(4) Chen, G. Q., and Gouaux, E. (1999) Probing the folding and unfolding of wild-type and mutant forms of bacteriorhodopsin in micellar solutions: Evaluation of reversible unfolding conditions. *Biochemistry 38*, 15380−15387.

(5) Lau, F. W., and Bowie, J. U. (1997) A method for assessing the stability of a membrane protein. *Biochemistry 36*, 5884−5892.

(6) Renthal, R. (2006) An unfolding story of helical transmembrane proteins. *Biochemistry 45*, 14559−14566.

(7) Anbazhagan, V., Cymer, F., and Schneider, D. (2010) Unfolding a transmembrane helix dimer: A FRET study in mixed micelles. *Arch. Biochem. Biophys. 495*, 159−164.

(8) Weber, M., Prodohl, A., Dreher, C., Becker, C., Underhaug, J., Svane, A. S., Malmendal, A., Nielsen, N. C., Otzen, D., and Schneider, D. (2011) SDS-Facilitated In vitro Formation of a Transmembrane B-Type Cytochrome Is Mediated by Changes in Local pH. *J. Mol. Biol. 407*, 594−606.

(9) Curnow, P., and Booth, P. J. (2007) Combined kinetic and thermodynamic analysis of $\alpha$-helical membrane protein unfolding. *Proc. Natl. Acad. Sci. U.S.A. 104*, 18970−18975.

(10) Otzen, D. E. (2003) Folding of DsbB in mixed micelles: A kinetic analysis of the stability of a bacterial membrane protein. *J. Mol. Biol. 330*, 641−649.

(11) Dutta, A., Tirupula, K. C., Alexiev, U., and Klein-Seetharaman, J. (2010) Characterization of membrane protein non-native states. 1. Extent of unfolding and aggregation of rhodopsin in the presence of chemical denaturants. *Biochemistry 49*, 6317−6328.

(12) Dutta, A., Kim, T. Y., Moeller, M., Wu, J., Alexiev, U., and Klein-Seetharaman, J. (2010) Characterization of membrane protein non-native states. 2. The SDS-unfolded states of rhodopsin. *Biochemistry 49*, 6329−6340.

(13) Fujiyoshi, Y., Mitsuoka, K., de Groot, B. L., Philippsen, A., Grubmuller, H., Agre, P., and Engel, A. (2002) Structure and function of water channels. *Curr. Opin. Struct. Biol. 12*, 509−515.

(14) Hara-Chikuma, M., and Verkman, A. S. (2006) Physiological roles of glycerol-transporting aquaporins: The aquaglyceroporins. *Cell. Mol. Life Sci. 63*, 1386−1392.

(15) Borgnia, M. J., and Agre, P. (2001) Reconstitution and functional comparison of purified GlpF and AqpZ, the glycerol and water channels from *Escherichia coli*. *Proc. Natl. Acad. Sci. U.S.A. 98*, 2888−2893.

(16) Galka, J. J., Baturin, S. J., Manley, D. M., Kehler, A. J., and O'Neil, J. D. (2008) Stability of the glycerol facilitator in detergent solutions. *Biochemistry 47*, 3513−3524.

(17) Cymer, F., and Schneider, D. (2010) A single glutamate residue controls the oligomerization, function, and stability of the aquaglyceroporin GlpF. *Biochemistry 49*, 279−286.

(18) Fu, D., Libson, A., Miercke, L. J., Weitzman, C., Nollert, P., Krucinski, J., and Stroud, R. M. (2000) Structure of a glycerol-conducting channel and the basis for its selectivity. *Science 290*, 481−486.

(19) Plasencia, I., Survery, S., Ibragimova, S., Hansen, J. S., Kjellbom, P., Helix-Nielsen, C., Johanson, U., and Mouritsen, O. G. (2011) Structure and stability of the spinach aquaporin SoPIP2;1 in detergent micelles and lipid membranes. *PLoS One 6*, e14674.

(20) Hansen, J. S., Vararattanavech, A., Plasencia, I., Greisen, P. J., Bomholt, J., Torres, J., Emneus, J., and Helix-Nielsen, C. (2011) Interaction between sodium dodecyl sulfate and membrane reconstituted aquaporins: A comparative study of spinach SoPIP2;1 and *E. coli* AqpZ. *Biochim. Biophys. Acta 1808*, 2600−2607.

(21) Pitonzo, D., and Skach, W. R. (2006) Molecular mechanisms of aquaporin biogenesis by the endoplasmic reticulum Sec61 translocon. *Biochim. Biophys. Acta 1758*, 976−988.

(22) Wu, C. S., and Chen, G. C. (1989) Adsorption of proteins onto glass surfaces and its effect on the intensity of circular dichroism spectra. *Anal. Biochem. 177*, 178−182.

(23) Fisher, L. E., Engelman, D. M., and Sturgis, J. N. (1999) Detergents modulate dimerization, but not helicity, of the glycophorin A transmembrane domain. *J. Mol. Biol. 293*, 639−651.

(24) Manley, D., and O'Neil, J. D. (2003) Preparation of glycerol facilitator for protein structure and folding studies in solution. *Methods Mol. Biol. 228*, 89−101.

(25) Robinson, P. J., and Pinheiro, T. J. (2009) The unfolding of the prion protein sheds light on the mechanisms of prion susceptibility and species barrier. *Biochemistry 48*, 8551−8558.

(26) Findlay, H. E., Rutherford, N. G., Henderson, P. J., and Booth, P. J. (2010) Unfolding free energy of a two-domain transmembrane sugar transport protein. *Proc. Natl. Acad. Sci. U.S.A. 107*, 18451−18456.

(27) Mi, D., Kim, H. J., Hadziselimovic, A., and Sanders, C. R. (2006) Irreversible misfolding of diacylglycerol kinase is independent of aggregation and occurs prior to trimerization and membrane association. *Biochemistry 45*, 10072−10084.

(28) Barrera, F. N., Renart, M. L., Poveda, J. A., de Kruijff, B., Killian, J. A., and Gonzalez-Ros, J. M. (2008) Protein self-assembly and lipid binding in the folding of the potassium channel KcsA. *Biochemistry 47*, 2123−2133.
(29) Di Bartolo, N. D., Hvorup, R. N., Locher, K. P., and Booth, P. J. (2011) In vitro folding and assembly of the *Escherichia coli* ATP-binding cassette transporter, BtuCD. *J. Biol. Chem. 286*, 18807−18815.
(30) Sanchez-Miguel, D. S., Romero-Jimenez, J., Reyes-Lopez, C. A., Cabrera-Avila, A. L., Carrillo-Ibarra, N., and Benitez-Cardoza, C. G. (2010) Chemical unfolding of enolase from *Saccharomyces cerevisiae* exhibits a three-state model. *Protein J. 29*, 1−10.
(31) Catanzano, F., Graziano, G., De Paola, B., Barone, G., D'Auria, S., Rossi, M., and Nucci, R. (1998) Guanidine-induced denaturation of *β*-glycosidase from *Sulfolobus solfataricus* expressed in *Escherichia coli*. *Biochemistry 37*, 14484−14490.
(32) Ptitsyn, O. B. (1995) Molten globule and protein folding. *Adv. Protein Chem. 47*, 83−229.
(33) Subramaniam, S., and Henderson, R. (2000) Molecular mechanism of vectorial proton translocation by bacteriorhodopsin. *Nature 406*, 653−657.
(34) Van Horn, W. D., Kim, H. J., Ellis, C. D., Hadziselimovic, A., Sulistijo, E. S., Karra, M. D., Tian, C., Sonnichsen, F. D., and Sanders, C. R. (2009) Solution nuclear magnetic resonance structure of membrane-integral diacylglycerol kinase. *Science 324*, 1726−1729.